Bitlis Eren Univ J Sci & Technol
3 (2), 39-43, 2013

ISSN 2146-7706

Research Article

Temperature dependent electronic properties of bulk Aluminium system

Koray Köksal [1,*], Fatih Ahmet Çelik [1], Fatih Koç [2]

[1] Department of Physics, Faculty of Arts and Science, Bitlis Eren University, TR 13000, Bitlis – Turkey
[2] Department of Physics, Science Institute, Bitlis Eren University, TR 13000, Bitlis – Turkey
** Corresponding author: kkoksal@beu.edu.tr*

Abstract

We investigate the possibility of controlling the electronic structure of the bulk aluminium material by given thermal energy to the system. As a bulk material, the structure and optical properties of the aluminium are well known in the literature. Its thermal dependent structural change has also been investigated many times. However, up to the best of our knowledge the relationship between the electronic properties, mechanical structure and some phase transitions of the aluminium due to the thermal energy pumping to the system has not been analyzed in detail. We show that the band structure of aluminium is strongly dependent on the thermal energy obtained by the system and on the phase transitions.

Keywords: metallic structures, electronic properties, molecular dynamics, optical properties

1. Introduction

The current studies on the bulk and nanomaterials show that the electronic properties can be controlled by external (Neto et al. 2009; Novoselov et al. 2004; Im et al. 2010; Goerbig 2011; Zou et al. 2012) or internal effects (Sahoo et al. 2011; Koksal et al. 2011). As an example on internal effects, recent studies proved that the absorption spectrum of a quantum dot is strongly dependent on its radius (Sahoo et al. 2011; Koksal et al. 2011). The external effects can be electric, magnetic, electro-magnetic fields or pressure and temperature.

While the small changes in the temperature result in the change of the motion of the electrons in the crystal structure due to the phonon-electron scattering, strong variations in temperature increases the vibration of lattices resulting in modification of the crystal structure (Patterson & Bailey 2005; Martin 2004). For some phase transitions, the lattice constants or volume of the structure change depending on the temperature (Cohen & Grest 1979). As well known, the band structure of the crystals is related to the volume and lattice constants (Harrison 2005). Therefore, it is possible to obtain the different band structure properties of the material for different temperatures. For a bulk system, the knowledge of the band structure is the most important information to investigate the macroscopic properties of the system like optical properties (Ashcroft & Sturm 1971; Stier et al. 1999). By using the information on the possible transitions between the electronic levels, it is also possible to easily calculate some experimental outcomes such as the dielectric function (Lautenschlager et al. 1987), refractive index (Gehrsitz et al. 2000) or PL spectrum (Li et al. 2003).

In order to see the effect of temperature on the optical properties, a theoretical study on Zn and Cd materials was introduced by Kasowski (1969). Johnson & Christy (1975) studied experimentally the temperature dependency of optical constants of Cu and Ni materials.

The temperature dependent optical properties of bulk Ag, Cu and Au materials were investigated by Winsemius et al. (1976) where the optical properties have been obtained experimentally and theoretically from the information on band structure for $T = 0\ K$. Jellison et al. (1983) experimentally analyzed the temperature dependent variation of the optical properties of silicon. Furthermore, the alloys such as AlN (Jiang et al. 2003), silicon carbide (Dakshinamurthy et al. 2007) and ZnO (Saha et al. 2009) have optical properties which are strongly dependent on the temperature. The crystallization properties of bulk aluminium material has been studied by Celik (2012) and the optical properties were experimentally investigated by Mathewson & Myers (1972).

In this study, we analyze the thermal dependency of band structure of bulk aluminium crystal. It has been shown with the help of simulation that, an aluminium crystal is heated up to the melting temperature to observe the possible phase transitions and the variation in lattice constant parameters or volume parameters. These temperature dependent parameters are used to obtain the band structure by using empirical pseudopotential technique.

2. Methods

2.1. Molecular dynamic simulation (MD)

In the past several years, the structural and electronic properties of metallic systems have been studied by using a variety of techniques. In particular, an experimental difficultly in the area can be overcome by using MD simulations. MD simulations based on the interatomic interactions are widely used to find the structural properties of metals or its alloys and amorphous systems (Tanaka 2005; Celik et al. 2008; Pei et al. 2005). The embedded atom method (EAM),

Received 5 October 2013
Available online December 2013

originally proposed by Daw & Baskes (1983) and Daw & Hatcher (1985), based on many body interactions has been used confidently in MD simulations on the metallic systems and used widely to solve many problems in bulk, surface and interface of metals and alloys. However, the EAM applications on the electronic, thermodynamic and structural properties of metallic systems have been increasing (Cagın et al. 1999; Kazanc 2007; Hui & Pederiva 2004). In this study, we have purposed to investigate the electronic and structural properties of bulk aluminium system during heating process by using MD simulations based on self consistent embedded atom method (SCEAM). The structure of the obtained solid and liquid phases has been analysed by using radial distribution function (RDF).

In the EAM formalism, the binding energy of an atom *i* in a crystal with N atoms is a sum of contributions from the pair potential and embedding potential functions. Various approaches have been applied to define EAM functions. Among those, the SCEAM approach is one of the simple approaches of the EAM, which has defined by incorporating the essential band character of metallic cohesion. In this approach the total crystal energy is calculated from

$$E_T = \sum_{i=1}^{N}\left[\frac{1}{2}\sum_{j\neq i}^{N}\left(\frac{a}{r_{ij}}\right)^n - c\sqrt{\bar{\rho}_i}\right] \tag{1}$$

$$\bar{\rho}_i = \sum_{j\neq i}^{N}\left(\frac{a}{r_{ij}}\right)^n \tag{2}$$

Here, *rij* is the distance between atoms *i* and *j*, *c* is a positive dimensionless parameter, ϵ is a parameter in dimension of energy, a is the lattice constant, and *m* and *n* are positive integers (Sutton & Chen 1990) which are determined by fitting to the experimental properties of material such as lattice constant (*a*), cohesive energy (*Ec*), and bulk modulus (*Bm*). The potential parameters for Al have been taken as *a* = 4.05 °*A*, *ε* = 33.147 *meV*, *c* = 16.399, *n* = 7 and *m* = 6 from Ozgen & Duruk (2004).

In this study, the MD method developed by Parrinello & Rahman (1981), which allows anisotropic volume change and so it can produce a NPH or NPT statistical ensembles, has been used. In the simulation studies, the equations of motion of the system were numerically solved by using the velocity version of Verlet algorithm with an integration step size of 2.35 *fs*. Potential energy functions were truncated at a distance of 2 a_0 (a_0 = 4.05 Å). The periodic boundary conditions were applied on the three dimensions of the MD cell. Time averages of the thermodynamic and structural properties of the systems in each simulation run were determined for 10000 integration steps following the equilibration of 2000 steps. The temperature of the systems has been controlled by rescaling the atomic velocities at every five integration steps. The simulation runs were applied for getting the equilibration of the system under zero pressure at 0 *K*, and then the temperature was increased from 0 *K* to 900 *K* with 50 *K* increment in each run of 10000 integration steps. At the temperature of 900 *K*, it has been observed that the system has a liquid phase, and so an extra 10000 steps were waited at 900 *K* to obtain relatively mixed liquid phase. The structures of the systems in solid and liquid phases were examined using the radial distribution function,

$$g(r) = \frac{V}{N^2}\left\langle\frac{\sum_i n_i(r)}{4\pi r^2\Delta r}\right\rangle \tag{3}$$

Where, $g(r)$ is the probability of finding of an atom in the range between r to $r + \Delta r$, the angular bracket denotes the time average. *N* is the number of atoms, $n_i(r)$ is the coordination number around atom *i* in the range from *r* to *r* + Δ*r*.

2.2. Band Structure Calculation

The electronic properties of the metallic structures can be determined by using empirical pseudopotential technique (EPM). The form factor is described by Cohen et al. (1966) as following

$$v(q) = -\left[\frac{4\pi Z e^2}{q^2\epsilon(q)\Omega}\cos(qR_c)\right] \tag{4}$$

where Ω is the atomic volume, *Rc* is core radius. The parameters such as volume and lattice constant can be obtained by molecular dynamic simulation. The procedure of the EPM technique can be written systematically. The Hamiltonian of a bulk metallic system is

$$\widehat{\mathbf{H}} = -\frac{\hbar^2}{2m_0}\nabla^2 + V_c(\mathbf{r}) \tag{5}$$

where *Vc* is the crystal potential which is felt by the electrons. The the Schrödinger’s equation reads

$$\widehat{\mathbf{H}}\psi_{n,\mathbf{k}} = E_{n,\mathbf{k}}\psi_{n,\mathbf{k}} \tag{6}$$

where the wavefunction is written as

$$\psi_{n,\mathbf{k}}(\mathbf{r}) = \sum_{\mathbf{G}} a_{n,\mathbf{k}}(\mathbf{G})u_{\mathbf{G},\mathbf{k}}$$

7)

where $u_{\mathbf{G};\mathbf{k}}$ is corresponding to the periodic lattice function as following

$$u_{\mathbf{G},\mathbf{k}} = \frac{1}{\sqrt{\Omega}}e^{i(\mathbf{G}+\mathbf{k})\mathbf{r}} \tag{8}$$

Therefore, the wavefunction becomes

$$\psi_{n,\mathbf{k}}(\mathbf{r}) = \frac{1}{\sqrt{\Omega}}\sum_{\mathbf{G}} a_{n,k}(\mathbf{G})e^{i(\mathbf{G}+\mathbf{k})\mathbf{r}} \tag{9}$$

Here, we can use the translational symmetry which is

$$\psi_{n,\mathbf{k}}(\mathbf{r}+\mathbf{R}) = e^{i\mathbf{k}.\mathbf{R}}\psi_{n,\mathbf{k}}(\mathbf{r}) \tag{10}$$

We can organize the Eq. 6 as following

$$\widehat{\mathbf{H}}\sum_{\mathbf{G}} a_{n,k}(\mathbf{G})u_{\mathbf{G},\boldsymbol{k}} = E\sum_{\mathbf{G}} a_{n,k}(\mathbf{G})u_{\mathbf{G},\boldsymbol{k}} \tag{11}$$

Further multiplying the above equation with $u^*_{\mathbf{G}',\mathbf{k}'}$ and integrated over r

$$\sum_{\mathrm{G}} a_{n,k}(\mathbf{G}) \int u^{*}_{\mathbf{G}',\mathbf{k}'} \widehat{\mathbf{H}}\, u_{\mathbf{G},\mathbf{k}} d\tau = \sum_{\mathrm{G}} a_{n,k}(\mathbf{G})\, E_{n,\mathbf{k}} \int u^{*}_{\mathbf{G}',\mathbf{k}'}\, u_{\mathbf{G},\mathbf{k}} d\tau \tag{12}$$

which results in

$$\sum_{\mathrm{G}} a_{n,k}(\mathbf{G}) \widehat{\mathbf{H}}_{\mathbf{G}',\mathbf{G}} = \sum_{\mathrm{G}} a_{n,k}(\mathbf{G}) E_{n,\mathbf{k}} \delta_{\mathbf{G}',\mathbf{G}} \tag{13}$$

where

$$\widehat{\mathbf{H}}_{\mathbf{G}',\mathbf{G}} = \int u^{*}_{\mathbf{G}',\mathbf{k}'} \widehat{\mathbf{H}}\, u_{\mathbf{G},\mathbf{k}} d\tau \tag{14}$$

and

$$\delta_{\mathbf{G}',\mathbf{G}} = \int u^{*}_{\mathbf{G}',\mathbf{k}'}\, u_{\mathbf{G},\mathbf{k}} d\tau \tag{15}$$

The last form of the hamiltonian can be written as

$$\widehat{\mathbf{H}}_{\mathbf{G}',\mathbf{G}} = \frac{\hbar^2}{2m_0} |\mathbf{G}+\mathbf{k}|^2 \delta_{\mathbf{G}',\mathbf{G}} + 2V_f(\mathbf{q}) \cos(\mathbf{G}-\mathbf{G}').\mathbf{T} \tag{16}$$

The calculation of the band structure of bulk copper material has been performed in the frame of this procedure. The detail of the procedure can be found in the literature (Harrison 2005). In addition to this calculations, we have used SIESTA software program to be sure that obtained band structure is trustable.

3. Results and Discussion

Molecular dynamic simulation has been performed to obtain the change in the mechanical properties of the aluminium crystal depending on the temperature. The temperature is increased from 0 K to 1000 K by 10 K steps. The change in lattice constant and volume with the change in temperature has been shown in Fig. 1.

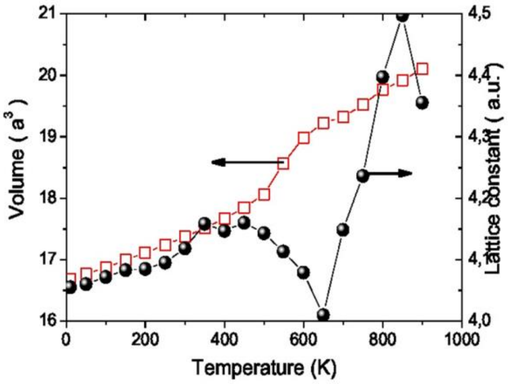

Figure 1. (Color online) The change in lattice constant and volume of the bulk aluminium crystal with increasing temperature. Red and black lines show the change in volume and lattice constants, respectively.

As can be seen from the figure, for $T \approx 700$ K, the lattice constant has a strong variation which indicates a phase transition. As expected, heating the sample leads to an increase in volume. Fig. 2 shows the radial distribution function of aluminium crystal for different temperature values. Radial distribution function is a perfect tool to analyze the crystal properties of the system. If the obtained peaks are sufficiently sharp, it can be said that the system is a crystal. As shown in Fig. 2, the curve at low temperatures has sharp peaks, while it becomes stable with the increase of the temperature. The effect of temperature, in this system, is to transform the structure from crystal phase to the amorphous.

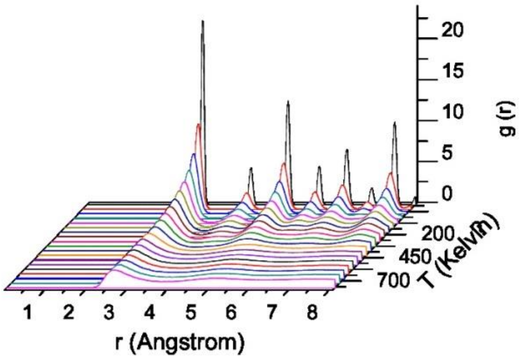

Figure 2. (Color online) The curves of radial distribution function during heating process.

The lattice constant and volume parameters are used to obtain electronic band structure of the aluminium material. Fig. 3 shows the change of the band structure with the change of the temperature, lattice constant and volume. In the subfigures, the zero point shows the fermi energy level. Fig. 3a shows the case of T = 0. The bandstructure is consistent with the literature and in this situation the material is a perfect crystal. When the temperature is increased to T = 150 K (Fig. 3b), the band structure and the position of fermi energy level change completely.

In the case of low temperature, curve has sharp peaks which indicates that the structure is a crystal. For higher temperature values, crystal structure turns into the amorphous one. The reason of the change can be understood from the Figs. 1 and 2. The heating deteriorates the perfect crystal structure of the material as seen from Fig. 2. Lattice volume of the material is also increasing. In the case of T = 250 K (Fig. 3c), the band structure shows different properties compared to that of

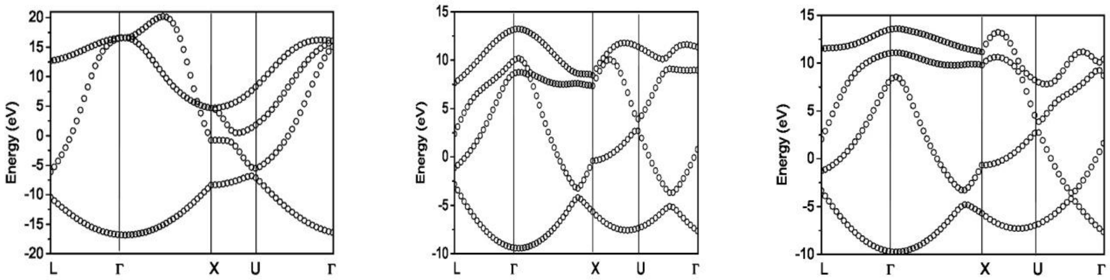

a) T=0 K b) T=150 K c) T=250 K

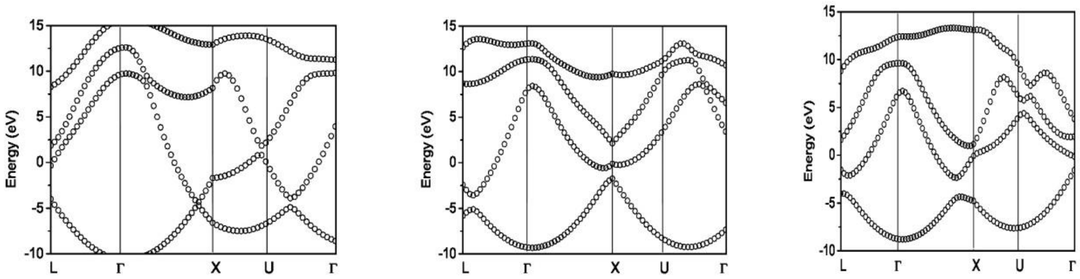

d) T=350 K e) T=450 K f) T=550 K

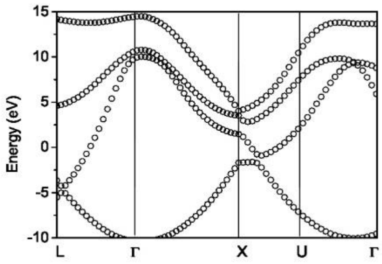

g) T=800 K

Figure 3. The band structure of the bulk aluminium changes with the variation of the temperature. The zero in energy is corresponding to the fermi energy level. *L*, Γ, *X*, *U* points show the symmetry points of the crystal.

T = 0 and T = 150 K, but the fermi energy level is at the same position with that of T = 150 K. In the case of T = 350 K (Fig. 3d), the fermi energy level has a little change and maximum and minimum energy values at Γ point are increasing. In the case of T = 450 K and T = 550 K (Figs. 3e and 3f) the subbands are separating from each other. And in the case of T = 800 K (Fig. 3g), non-degenerate subbands (specifically at Γ point) are showing up. It should be noticed that these results of band structure are not convenient to directly compare with the experimental results, but it can lead to make some comments. However, this study contributes to the literature by introducing the temperature dependent band structures without consideration of optical properties of the system.

The zero in energy is corresponding to the fermi energy level. L, Γ, X, U points show the symmetry points of the crystal.

4. Conclusion

We have investigated the possibility of the control of band structure of the bulk materials by introducing the thermal parameters to the system. Here, we would like to notice that the optical and electronic properties are completely related to the band structure of the system. With the possibility of important modifications of the band structure by variation of temperature, one can be able to obtain a chance to change the optical and electronic properties of the system. This study is a part of a project about the dependency of the bulk and nanomaterials on thermal properties of the system.

Furthermore, the variation of band structure leads to change in dielectric function and related optical properties. The change in mechanical structure of the system has been analyzed by molecular dynamic simulation. Band structure calculation has been performed by empirical pseudopotential technique.

Acknowledgements

This work is supported by the TUBİTAK through Project No 112T991.

References

Ashcroft N, Sturm K (1971). Interband Absorption and the Optical Properties of Polyvalent Metals. Phys Rev B 3, 1898.

Cagın T, Dereli G, Uludogan M, Tomak M (1999). Thermal and mechanical properties of some fcc transition metals. Phys Rev B 59, 3468.

Celik F, Kazanc S, Yildiz A, Ozgen S (2008). Pressure effect on the structural properties of amorphous Ag during isothermal annealing. Intermetallics 16, 793.

Celik FA (2012). Molecular dynamics simulation of crystallization of amorphous aluminium modelled with EAM. Bitlis Eren Univ J Sci Technol 2, 44-48.

Cohen MH, Grest GS (1979). Liquid-glass transition, a free-volume approach. Phys Rev B 20, 1077.

Cohen ML, Bergstresser TK (1966). Band structures and pseudopotential form factors for fourteen semiconductors of the diamond and zinc-blende structures. Phys Rev 141, 789.

Dakshinamurthy S, Quick N, Kar A (2007). Temperature-dependent optical properties of silicon carbide for wireless temperature sensors. J Phys Appl Phys 40, 353.

Daw MS, Baskes M (1983). Semiempirical, quantum mechanical calculation of hydrogen embrittlement in metals. Phys Rev Lett 50, 1285.

Daw MS, Hatcher R (1985). Application of the embedded atom method to phonons in transition metals. Solid State Comm 56, 697.

Gehrsitz S, Reinhart F, Gourgon C, Herres N, Vonlanthen A, Sigg H (2000). The refractive index of AlxGa1−xAs below the band gap: Accurate determination and empirical modeling. J Appl Phys 87, 7825.

Goerbig M (2011). Electronic properties of graphene in a strong magnetic field. Rev Mod Phys 83, 1193.

Harrison P (2005). Quantum wells, wires and dots: theoretical and computational physics of semiconductor nanostructures. John Wiley & Sons, 564 p. ISBN: 978-0-470-77098-6.

Hui L, Pederiva F (2004). Structural study of local order in quenched lead under high pressures. Chem Phys 304, 261.

Im J, Cho E, Kim D, Horii H, Ihm J, Han S (2010). Effects of pressure on atomic and electronic structure and crystallization dynamics of amorphous $Ge_2Sb_2Te_5$. Phys Rev B 81, 245211.

Jellison Jr G, Lowndes D, Wood R (1983). Importance of temperature-dependent optical properties for Raman-temperature measurements for silicon. Phys Rev B 28, 3272.

Jiang L, Shen W, Ogawa H, Guo Q (2003). Temperature dependence of the optical properties in hexagonal AlN. J Appl Phys 94, 5704.

Johnson P, Christy R (1975). Optical constants of copper and nickel as a function of temperature. Phys Rev B 11, 1315.

Kasowski R (1969). Temperature-dependent optical properties of Zn and Cd: A theoretical study. Phys Rev 187, 885.

Kazanc S (2007). Molecular dynamics study of pressure effect on crystallization behaviour of amorphous CuNi alloy during isothermal annealing. Phys Lett A 365, 473.

Koksal K, Berakdar J, Pavlyukh Y (2011). Metal spherical nanostructures and dielectric response quantum-size effects in silver nanoclusters. Bitlis Eren Univ J Sci Technol 1, 4-6.

Lautenschlager P, Garriga M, Vina L, Cardona M (1987). Temperature dependence of the dielectric function and interband critical points in silicon. Phys Rev B 36, 4821.

Li J, Nam K, Nakarmi M, Lin J, Jiang H, Carrier P, Wei S-H (2003). Band structure and fundamental optical transitions in wurtzite AlN. Appl Phys Lett 83, 5163.

Martin RM (2004). Electronic Structure: Basic Theory and Practical Methods, Cambridge University Press, 624 p., ISBN 9780521782852,

Mathewson A, Myers H (1972). Optical absorption in aluminium and the effect of temperature. J Phys F Met Phys 2, 403.

Neto AC, Guinea F, Peres N, Novoselov K, Geim A (2009). The electronic properties of graphene. Rev Mod Phys 81, 109.

Novoselov K, Geim AK, Morozov S, Jiang D, Zhang Y, Dubonos S, Grigorieva I, Firsov A (2004). Electric field effect in atomically thin carbon films. Science 306, 666.

Ozgen S, Duruk E (2004). Molecular dynamics simulation of solidification kinetics of aluminium using Sutton–Chen version of EAM. Mater Lett 58, 1071.

Parrinello M, Rahman A (1981). Polymorphic transitions in single crystals: A new molecular dynamics method. J Appl Phys 52, 7182.

Patterson J, Bailey B (2005). Solid-State Physics: Introduction to the Theory, 813 p., Springer, ISBN 978-3-642-02588-4.

Pei Q, Lu C, Lee H (2005). Crystallization of amorphous alloy during isothermal annealing: a molecular dynamics study. J Phys Condens Matter 17, 1493.

Saha S, Mehan N, Sreenivas K, Gupta V (2009). Temperature dependent optical properties of (002) oriented ZnO thin film using surface plasmon resonance. Appl Phys Lett 95, 071106.

Sahoo SK, Pal S, Sarkar P, Majumder C (2011). Size-dependent electronic structure of rutile TiO_2 quantum dots. Chem Phys Lett 516, 68.

Stier O, Grundmann M, Bimberg D (1999). Electronic and optical properties of strained quantum dots modeled by 8-band k·p theory. Phys Rev B 59, 5688.

Sutton A, Chen J (1990). Long-range Finnis–Sinclair potentials. Phil Mag Lett 61, 139.

Tanaka H (2005). Relationship among glass-forming ability, fragility, and short-range bond ordering of liquids. J Non-crystalline solid 351, 678.

Winsemius P, Kampen FV, Lengkeek H, Went CV (1976). Temperature dependence of the optical properties of Au, Ag and Cu. J Phys F Met Phys 6, 1583.

Zou C, Fan L, Chen R, Yan X, Yan W, Pan G, Wu Z, Gao W (2012). Thermally driven V_2O_5 formation and the temperature-dependent electronic structure study. Cryst Eng Comm 14, 626.